Fault Location on Series-Compensated Transmission Line Using Measurements of Current Differential Protective Relays

M.M. Saha
ABB, AB
Västerås, Sweden
murari.saha@se.abb.com

J. Izykowski, E. Rosolowski
Wroclaw University of Technology
Wroclaw, Poland
jan.izykowski@pwr.wroc.pl,
eugeniusz.rosolowski@pwr.wroc.pl

***Abstract*—An accurate algorithm for locating faults on a series-compensated line is presented. This algorithm can be applied with current differential protective relays since two-end currents and one-end voltage are utilized as the fault locator input signals. The algorithm applies two subroutines and the procedure for indicating the valid subroutine. The algorithm has been evaluated using the fault data of ATP-EMTP versatile simulations of faults on a series-compensated transmission line. The presented example shows the validity of the presented algorithm and its high accuracy.**

Keywords-transmission line; series compensation; fault location; current differential protective relay

I. INTRODUCTION

When a fault occurs on an overhead line, it is very important for the utility to identify the fault location as quickly as possible for improving the service reliability. If a fault location cannot be identified quickly then a prolonged line outage during a period of peak load and severe economic losses may occur, leading to questioning of the reliability of service. All these circumstances have raised the great importance of fault location for the inspection-repair purpose. It is so especially for series-compensated lines spreading over few hundreds of kilometers and being vital links between the energy production and consumption centers [1]–[8].

The method based on an impedance principle, making use of the fundamental-frequency voltages and currents is the most popular for fault location. In particular, in [3, 6], the algorithms utilizing one-end current and voltage measurements for application to series-compensated lines have been presented. In [7] use of two-end currents and voltages, measured synchronously [9] with the aid of PMUs, has been considered. In turn, application of the two-end unsynchronized measurements has been considered in [5]. Also the knowledge-based approaches have been proposed for the fault location purpose, as for example as in [2].

In this paper a specific fault location algorithm for a series-compensated line is presented. The distance to fault is determined using two-end currents, while voltage from only one-end of the line. Utilization of such fault locator input signals becomes the case when one incorporates the fault locator into a current differential protective relay (Fig. 1: the fault locator FL_A incorporated into the relay DIFF REL_A).

The presented fault location algorithm is designated for application to a single-circuit (Fig. 1a) or a double-circuit (Fig. 1b) series-compensated line. It is considered that the compensation is performed with use of three-phase bank of fixed series capacitors (SCs) installed at midpoint of the line. The SCs are equipped with MOVs (Metal Oxide Varistors) for overvoltage protection. The MOVs are protected from overheating by a thermal protection (TP) – Fig. 1a (note that for the sake of simplicity this protection is not included in all next drawings).

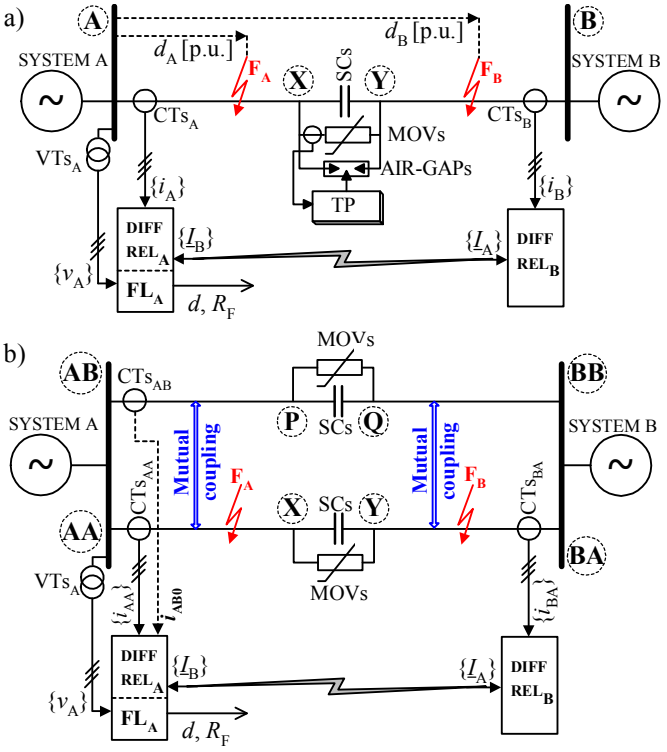

Figure 1. Schematic diagram for fault locator FL_A associated with current differential protective relays of series-compensated line: a) single-circuit line, b) double-circuit line.

A fault location algorithm is further derived for the case of a single-circuit line (Fig. 1a). The fault locator (FL_A) is supplied from CTs_A, VTs_A measuring three-phase current $\{i_A\}$ and voltage $\{v_A\}$ at the bus A. Additionally, the phasors of three-phase current $\{\underline{I}_B\}$ measured at the remote bus B are provided via the communication channel of the differential relays.

In the case of a double-circuit line (Fig. 1b) one needs additionally to compensate for a mutual coupling of parallel lines and thus a zero-sequence current from the healthy parallel line (i_{AB0}) has to be available for the fault locator.

II. FAULT LOCATION ALGORITHM

A fault is of a random nature and therefore one needs to consider the faults appearing at both sides of the three-phase capacitor compensating bank – Fig. 1a: faults F_A and F_B. In consequence, two subroutines: SUB_A, SUB_B are utilized for locating these hypothetical faults. In addition, the selection procedure is applied for indicating the valid subroutine yielding the result consistent with the actual fault.

The compensating bank divides the line of the length ℓ [km] into two line segments having the length: d_{SC} [p.u.] and $(1-d_{SC})$ [p.u.], as shown in Figs. 2 and 3. First, the subroutines SUB_A (Fig. 2), SUB_B (Fig. 3) yield the per unit distance to fault: d_{FA}, d_{FB}, each related to the length of the particular line segment: ($d_{SC}\ell$) or $(1-d_{SC})\ell$. Finally, one recalculates the relative distances d_{FA}, d_{FB} into the distances: d_A, d_B which are also expressed in [p.u.], but related to the whole line length:

$$d_A = d_{FA} \cdot d_{SC} \tag{1}$$

$$d_B = d_{SC} + (1-d_{FB}) \cdot (1-d_{SC}) \tag{2}$$

A. Fault location subroutine SUB_A

The subroutine SUB_A is here derived under neglecting the line shunt capacitances effect, however, it can be accounted for in the next step.

The subroutine SUB_A for fault F_A in the section A–X is based on the following generalized fault loop model [4]:

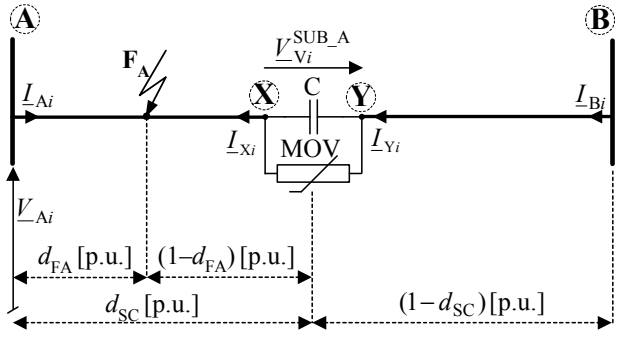

Figure 2. Subroutine SUB_A – scheme of series-compensated line under fault F_A for *i*th symmetrical component.

$$\underline{V}_{Ap} - d_{FA}\underline{Z}_{1LA}\underline{I}_{Ap} - R_{FA}\underline{I}_{FA} = 0 \tag{3}$$

where:

d_{FA} – unknown distance to fault [p.u.] on the section A–X;

R_{FA} – unknown fault resistance;

$\underline{V}_{Ap}$, $\underline{I}_{Ap}$ – fault loop voltage and current;

$\underline{I}_{FA}$ – total fault current (fault path current);

$\underline{Z}_{1LA}$ – positive-sequence impedance of the line section A–X;
Note: $\underline{Z}_{1LA} = d_{SC}\underline{Z}_{1L}$, where: $\underline{Z}_{1L}$ – positive-sequence impedance of the whole line.

Fault loop voltage and current, composed accordingly to the fault type, are expressed as follows [4]:

$$\underline{V}_{Ap} = \underline{a}_1\underline{V}_{A1} + \underline{a}_2\underline{V}_{A2} + \underline{a}_0\underline{V}_{A0} \tag{4}$$

$$\underline{I}_{Ap} = \underline{a}_1\underline{I}_{A1} + \underline{a}_2\underline{I}_{A2} + \underline{a}_0\frac{\underline{Z}_{0LA}}{\underline{Z}_{1LA}}\underline{I}_{A0} \tag{5}$$

where:

$\underline{a}_1$, $\underline{a}_2$, $\underline{a}_0$ – weighting coefficients (Table I);

$\underline{V}_{A1}$, $\underline{V}_{A2}$, $\underline{V}_{A0}$ – symmetrical components (positive-, negative- and zero-sequence) of voltage from the bus A;

$\underline{I}_{A1}$, $\underline{I}_{A2}$, $\underline{I}_{A0}$ – symmetrical components of the bus A currents;

$\underline{Z}_{0LA}$ – zero-sequence impedance of the line section A–X.

It is proposed to determine the total fault current from (3) using the following generalized fault model [8]:

$$\underline{I}_{FA} = \underline{a}_{F1}\underline{I}_{FA1} + \underline{a}_{F2}\underline{I}_{FA2} + \underline{a}_{F0}\underline{I}_{FA0} \tag{6}$$

where:

$\underline{a}_{F1}$, $\underline{a}_{F2}$, $\underline{a}_{F0}$ – share coefficients (Table II).

The *i*th sequence component of the total fault current is determined as a sum of the *i*th sequence components of currents from both ends of the faulted section A–X:

$$\underline{I}_{FAi} = \underline{I}_{Ai} + \underline{I}_{Xi} \tag{7}$$

where:

i=1–positive-, *i*=2–negative-, *i*=0–zero-sequence component

$\underline{I}_{Ai}$ – *i*th sequence component of current at the bus A;

$\underline{I}_{Xi}$ – *i*th sequence component of current at the point X. When neglecting the line shunt capacitances it is equal to the current $\underline{I}_{Bi}$, and thus one obtains:

$$\underline{I}_{\mathrm{FA}i} = \underline{I}_{\mathrm{A}i} + \underline{I}_{\mathrm{B}i} \tag{8}$$

In order to assure possibly highest accuracy of fault location, the following priority for usage of particular sequence components, as in Table II, was proposed:

- *for phase-to-ground and phase-to-phase faults*: use of negative-sequence components;
- *for phase-to-phase-to-ground faults*: use of negative- and zero-sequence components;
- *for three phase symmetrical faults*: use of incremental positive-sequence components.

In the case of three-phase balanced faults the total fault current is determined taking the incremental positive-sequence currents from both line ends A, B, respectively:

$$\underline{I}_{\mathrm{FA1}} = \underline{I}_{\mathrm{A1}}^{\mathrm{incr.}} + \underline{I}_{\mathrm{B1}}^{\mathrm{incr.}} \tag{9}$$

where the incremental (superscript: 'incr.') positive-sequence currents are calculated by subtracting the pre-fault quantity (the superscript: 'pre') from the fault quantity:

$$\underline{I}_{\mathrm{FA1}} = (\underline{I}_{\mathrm{A1}} - \underline{I}_{\mathrm{A1}}^{\mathrm{pre}}) + (\underline{I}_{\mathrm{B1}} - \underline{I}_{\mathrm{B1}}^{\mathrm{pre}}) \tag{10}$$

TABLE I. COEFFICIENTS FOR COMPOSING SIGNALS (4)–(5)

Fault type	$\underline{a}_1$	$\underline{a}_2$	$\underline{a}_0$
a–E	1	1	1
b–E	$-0.5 - \mathrm{j}0.5\sqrt{3}$	$-0.5 + \mathrm{j}0.5\sqrt{3}$	1
c–E	$-0.5 + \mathrm{j}0.5\sqrt{3}$	$-0.5 - \mathrm{j}0.5\sqrt{3}$	1
a–b, a–b–E a–b–c, a–b–c–E	$1.5 + \mathrm{j}0.5\sqrt{3}$	$1.5 - \mathrm{j}0.5\sqrt{3}$	0
b–c, b–c–E	$-\mathrm{j}\sqrt{3}$	$\mathrm{j}\sqrt{3}$	0
c–a, c–a–E	$-1.5 + \mathrm{j}0.5\sqrt{3}$	$-1.5 - \mathrm{j}0.5\sqrt{3}$	0

TABLE II. SHARE COEFFICIENTS USED IN FAULT MODEL (6)

Fault type	$\underline{a}_{\mathrm{F1}}$	$\underline{a}_{\mathrm{F2}}$	$\underline{a}_{\mathrm{F0}}$
a–E	0	3	0
b–E	0	$-1.5 + \mathrm{j}1.5\sqrt{3}$	0
c–E	0	$-1.5 - \mathrm{j}1.5\sqrt{3}$	0
a–b	0	$1.5 - \mathrm{j}0.5\sqrt{3}$	0
b–c	0	$\mathrm{j}\sqrt{3}$	0
c–a	0	$-1.5 - \mathrm{j}0.5\sqrt{3}$	0
a–b–E	0	$3 - \mathrm{j}\sqrt{3}$	$\mathrm{j}\sqrt{3}$
b–c–E	0	$\mathrm{j}2\sqrt{3}$	$\mathrm{j}\sqrt{3}$
c–a–E	0	$3 + \mathrm{j}\sqrt{3}$	$\mathrm{j}\sqrt{3}$
a–b–c a–b–c–E	$1.5 + \mathrm{j}0.5\sqrt{3}$	$1.5 - \mathrm{j}0.5\sqrt{3}$ *)	0
*) $\underline{a}_{\mathrm{F2}} \neq 0$ and there is no negative-sequence component			

In this way, an accurate calculation of the total fault current is assured since the positive-sequence components, for which the shunt capacitance effect is the most distinct, are excluded for all fault types (Table II).

After resolving (3) into the real and imaginary parts and then eliminating the unknown fault resistance (R_{FA}), the sought fault distance (d_{FA}) is determined as follows:

$$d_{\mathrm{FA}} = \frac{\mathrm{real}(\underline{V}_{\mathrm{Ap}})\,\mathrm{imag}(\underline{I}_{\mathrm{FA}}) - \mathrm{imag}(\underline{V}_{\mathrm{Ap}})\,\mathrm{real}(\underline{I}_{\mathrm{FA}})}{\mathrm{real}(\underline{Z}_{\mathrm{1LA}}\,\underline{I}_{\mathrm{Ap}})\,\mathrm{imag}(\underline{I}_{\mathrm{FA}}) - \mathrm{imag}(\underline{Z}_{\mathrm{1LA}}\,\underline{I}_{\mathrm{Ap}})\,\mathrm{real}(\underline{I}_{\mathrm{FA}})} \tag{11}$$

Having the fault distance calculated (11), the fault resistance R_{FA} can be also determined.

B. Fault location subroutine SUB_B

Transferring the *i*th symmetrical sequence current from the beginning of the line section (bus A) to the end point (X) of the un-faulted section A–X (Fig. 3) gives:

$$\underline{I}_{\mathrm{X}i} = \frac{-\sinh(\underline{\gamma}_i d_{\mathrm{SC}}\ell)\cdot\underline{V}_{\mathrm{A}i}}{\underline{Z}_{ci}} + \cos(\underline{\gamma}_i d_{\mathrm{SC}}\ell)\cdot\underline{I}_{\mathrm{A}i} \tag{13}$$

If there is no internal fault in the compensating bank, then at both sides of the bank we have identical currents (Fig. 3):

$$\underline{I}_{\mathrm{Y}i} = \underline{I}_{\mathrm{X}i} \tag{14}$$

Transferring the voltage from the bus A towards the compensating bank, up to the point X (Fig. 3), gives:

$$\underline{V}_{\mathrm{X}i} = \underline{V}_{\mathrm{A}i}\cosh(\underline{\gamma}_i d_{\mathrm{SC}}\ell) - \underline{Z}_{ci}\,\underline{I}_{\mathrm{A}i}\sinh(\underline{\gamma}_i d_{\mathrm{SC}}\ell) \tag{12}$$

where:

$\underline{Z}_{ci} = \sqrt{\underline{Z}'_{i\mathrm{L}}/\underline{Y}'_{i\mathrm{L}}}$, $\underline{\gamma}_i = \sqrt{\underline{Z}'_{i\mathrm{L}}\,\underline{Y}'_{i\mathrm{L}}}$ – surge impedance and propagation constant of the line for the *i*th sequence;

$\underline{Z}'_{i\mathrm{L}}$, $\underline{Y}'_{i\mathrm{L}}$ – impedance (Ω/km) and admittance (S/km) of the line for the *i*th sequence.

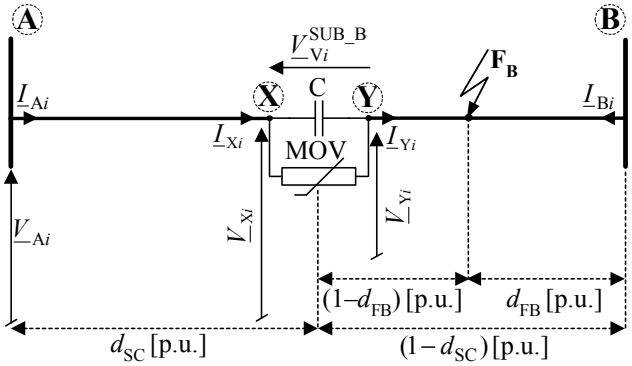

Figure 3. Subroutine SUB_B – scheme of series-compensated line under fault $\mathrm{F_B}$ for the *i*th symmetrical component.

In contrast, at both sides of the compensating bank there is a different voltage due to presence of voltage drops across the SC&MOV in particular phases. These voltage drops can be calculated with use of the fundamental frequency equivalent impedance Z_V, consisting of the resistance R_V and reactance X_V – connected in series [6], as follows:

$$\underline{V}_{V\_j}^{SUB\_B} = \underline{Z}_{V\_j}(|\underline{I}_{X\_j}|)\cdot\underline{I}_{X\_j} \tag{15}$$

where:

$\underline{I}_{X\_j}$ – phasors of the currents flowing through the SC&MOV in phase j (phases are marked as: j=a, b or c);

$|\underline{X}|$ denotes the amplitude of the phasor $\underline{X}$.

The ith sequence of voltage at the point Y is determined as:

$$\underline{V}_{Yi} = \underline{V}_{Xi} - \underline{V}_{Vi}^{SUB\_B} \tag{16}$$

where:

$\underline{V}_{Vi}^{SUB\_B}$ – voltage drop across the compensating bank for the ith sequence, obtained from the drops in phases: j=a, b, c (15).

In the considered case of the subroutine SUB_B, the generalized model describes the fault loop seen from the point Y towards the fault point F_B (Fig. 3):

$$\underline{V}_{FBp}(d_{FB}) - R_{FB}\underline{I}_{FB}(d_{FB}) = 0 \tag{17}$$

where:

$\underline{V}_{FBp}(d_{FB})$ – fault loop voltage, composed accordingly to the fault type, obtained after the analytic transfer of this voltage from the point Y to the fault point F_B;

R_{FB} – unknown fault path resistance;

$\underline{I}_{FB}(d_{FB})$ – total fault current (fault path current).

The fault loop voltage transferred from Y to F_B can be composed as the following weighted sum of the respective symmetrical components of voltage:

$$\underline{V}_{FBp}(d_{FB}) = \underline{a}_1\underline{V}_{FB1}(d_{FB}) + \underline{a}_2\underline{V}_{FB2}(d_{FB}) + \underline{a}_0\underline{V}_{FB0}(d_{FB}) \tag{18}$$

where: $\underline{a}_1$, $\underline{a}_2$, $\underline{a}_0$ – weighting coefficients, as in Table I.

Applying the distributed parameter line model, the ith symmetrical component of voltages from (18) are determined as follows:

$$\begin{aligned}\underline{V}_{FBi} = {} & \underline{V}_{Yi}\cosh(\underline{\gamma}_i(1-d_{SC})\ell(1-d_{FB})) \\ & - \underline{Z}_{ci}\underline{I}_{Yi}\sinh(\underline{\gamma}_i(1-d_{SC})\ell(1-d_{FB}))\end{aligned} \tag{19}$$

where:

$\underline{V}_{Yi}$ – symmetrical components of voltage at the point Y, determined in (16);

$\underline{I}_{Yi}$ – symmetrical components of current at the point Y, determined in (13)–(14).

Analogously as in (6) for the subroutine SUB_A, the total fault current ($\underline{I}_{FB}$) can be expressed as the following combination of its symmetrical components:

$$\underline{I}_{FB}(d_{FB}) = \underline{a}'_{F1}\underline{I}_{FB1}(d_{FB}) + \underline{a}'_{F2}\underline{I}_{FB2}(d_{FB}) + \underline{a}'_{F0}\underline{I}_{FB0}(d_{FB}) \tag{20}$$

where:

$\underline{a}'_{F1}$, $\underline{a}'_{F2}$, $\underline{a}'_{F0}$ – share coefficients. The recommended set of these coefficients is delivered in Table III and differs from that for the subroutine SUB_A presented in Table II.

Taking into account that the zero-sequence is eliminated (Table III: $\underline{a}'_{F0} = 0$ for all fault types), one obtains the total fault current [4] in the form:

$$\underline{I}_{FB}(d_{FB}) = \frac{\underline{a}'_{F1}\underline{M}_1 + \underline{a}'_{F2}\underline{M}_2}{\cosh(\underline{\gamma}_1(1-d_{SC})\ell d_{FB})} \tag{21}$$

where:

$\underline{M}_i = \underline{I}_{Bi} + \underline{I}_{Yi}\cosh(\underline{\gamma}_1(1-d_{SC})\ell) - \frac{\underline{V}_{Yi}}{\underline{Z}_{c1}}\sinh(\underline{\gamma}_1(1-d_{SC})\ell)$;

and where:

i=1: positive-sequence or i=2: negative-sequence.

Substitution of the total fault current (21) into the generalized fault loop model (17) gives:

$$\underline{V}_{FBp}(d_{FB}) - R_{FB}\frac{\underline{a}'_{F1}\underline{M}_1 + \underline{a}'_{F2}\underline{M}_2}{\cosh(\underline{\gamma}_1(1-d_{SC})\ell d_{FB})} = 0 \tag{22}$$

where the involved quantities are defined in (18)–(19), (21), while the coefficients are gathered in Table III.

TABLE III. SHARE COEFFICIENTS USED FOR COMPOSING CURRENT (20)

Fault type	$\underline{a}'_{F1}$	$\underline{a}'_{F2}$	$\underline{a}'_{F0}$
a–E	0	3	0
b–E	0	$-1.5+j1.5\sqrt{3}$	0
c–E	0	$-1.5-j1.5\sqrt{3}$	0
a–b	0	$1.5-j0.5\sqrt{3}$	0
b–c	0	$j\sqrt{3}$	0
c–a	0	$-1.5-j0.5\sqrt{3}$	0
a–b–E	$1.5+j0.5\sqrt{3}$	$1.5-j0.5\sqrt{3}$	0
b–c–E	$-j\sqrt{3}$	$j\sqrt{3}$	0
c–a–E	$-1.5+j0.5\sqrt{3}$	$-1.5-j0.5\sqrt{3}$	0
a–b–c, a–b–c–E	$1.5+j0.5\sqrt{3}$	$1.5-j0.5\sqrt{3}$ *)	0

*) – there is no negative-sequence component under these faults and the coefficient can be assumed as equal to zero

The derived fault location formula (22) is compact and covers different fault types, what requires setting the appropriate fault type coefficients provided in Tables I and III. There are two unknowns in (22): distance to fault d_{FB} and fault resistance R_{FB}. After resolving (22) into the real and imaginary parts, one of the known numeric procedures for solving nonlinear equations can be applied. It has been checked that the Newton-Raphson iterative method is a good choice for that.

C. *Selection procedure*

First, the subroutine yielding the distance to fault outside the section range and/or the fault resistance of negative value is rejected. In vast majority of the cases this allows to select the valid subroutine. If this is not so, then one has to proceed with further selection. For this purpose, the circuit diagrams of the network for the negative-sequence, relevant for both subroutines are considered. In the case of three-phase balanced faults the incremental positive-sequence components are considered. The particular subroutine is selected as the valid one if the determined remote source impedance ($\underline{Z}_{1SB}^{SUB\_A}$ or $\underline{Z}_{1SB}^{SUB\_B}$) has an *R–L* character and its value is close to the actual source impedance: $\underline{Z}_{1SB}$.

D. *Improvement of fault location accuracy*

The subroutine SUB_A (Section IIA) does not require knowing parameters of the compensating bank. In contrast, the subroutine SUB_B (Section IIB) applies a transfer of the voltage across the compensating bank. Thus, a possible error in making this transfer, due to uncertainty with respect to the parameters of the compensating bank , influences accuracy of fault location for the subroutine SUB_B. In order to improve fault location accuracy, one can incorporate the fault location function into current differential protective relays at both ends of the line. As a result, the distance to both faults (F_A, F_B) are calculated without involving parameters of the series capacitor bank. However, those parameters are required only when deciding whether the fault locator FL_A or FL_B yields the results (distance to fault and fault resistance) consistent with the actual fault.

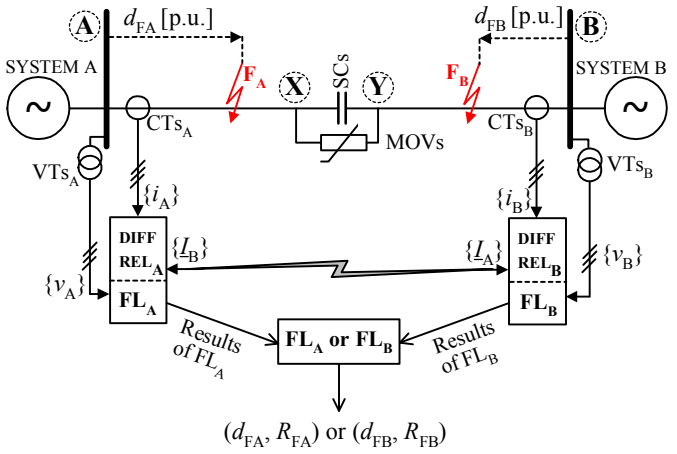

Figure 4. Incorporation of fault location function into current differential protective relays at both line ends.

III. ATP-EMTP EVALUATION

The 300-km, 400-kV transmission line compensated in the middle (d_{SC}=0.5 p.u.), at the degree of 70%, was modeled using ATP-EMTP software [10]. The line impedances were assumed as equal to:
$\underline{Z}_{1L}$=(8.28+j94.5) Ω, $\underline{Z}_{0L}$=(82.5+j307.9) Ω,
and the line shunt capacitances:
C_{1L}=13 nF/km, C_{0L}=8.5 nF/km.

The supplying systems (System A and System B) were modeled with the impedances:
$\underline{Z}_{1SA}$=$\underline{Z}_{1SB}$=(1.31+j15)Ω, $\underline{Z}_{0SA}$=$\underline{Z}_{0SB}$=(2.33+j22.5) Ω;

The e.m.f. of the System B were delayed by 10° with respect to the System A.

The MOVs with the common approximation $i = P(v/V_{REF})^q$ were modeled taking: P=1 kA, V_{REF}=150 kV, q=23. The model includes the Capacitive Voltage Transformers (CVTs) and the Current Transformers (CTs).

The analog filters with 350 Hz cut-off frequency were included. The sampling frequency of 1000 Hz was applied and the phasors were determined using the DFT algorithm.

Fig. 5 presents the results for the example fault – fault type: a–g; fault distance: d_B=0.833 p.u. (the fault behind the compensating bank, as seen from the bus A – thus the subroutine SUB_B will yield the correct results); fault resistance: R_{FB}=25 Ω. The continuous results were averaged within the fault period ($30 \div 50$) ms. Both subroutines indicate the fault as occurring within their line sections:

- SUB_A: $d_A = 0.4208$ p.u. $< d_{SC}$ p.u. (section A–X);
- SUB_B: $d_B = 0.8281$ p.u. $> d_{SC}$ p.u. (section Y–B).

The fault resistance values (Fig. 5b) are positive too:

- SUB_A: R_{FA}=43.93 Ω;
- SUB_B: R_{FB}=24.44 Ω.

Continuing the selection, the remote source impedance values relevant for both subroutines: $\underline{Z}_{1SB}^{SUB\_A}$, $\underline{Z}_{1SB}^{SUB\_B}$ have been calculated (Table IV).

a)

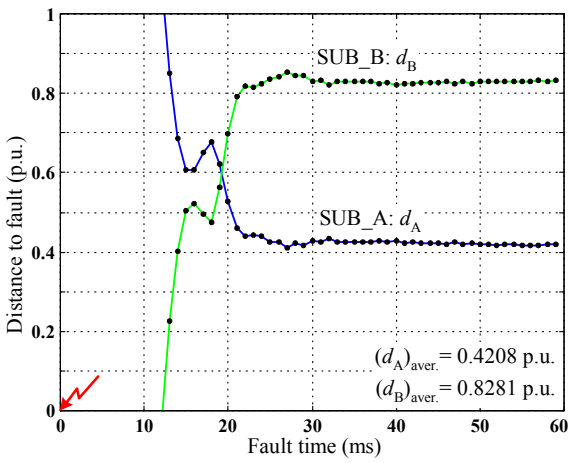

b)

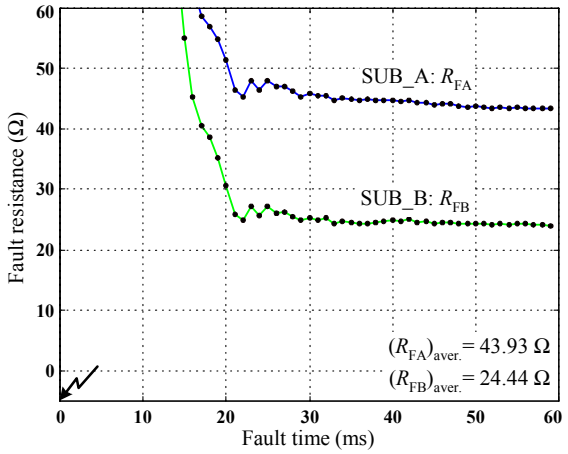

Figure 5. Fault location example: a) distance to fault, b) fault resistance.

TABLE IV. FAULT LOCATION EXAMPLE – SELECTION OF VALID SUBROUTINE ON BASE OF ESTIMATED REMOTE SOURCE IMPEDANCE.

Remote source impedance			Valid Subroutine:
Actual:	Estimated:		
$\underline{Z}_{1SB}$	$\underline{Z}_{1SB}^{SUB\_A}$	$\underline{Z}_{1SB}^{SUB\_B}$	
1.31+j15	–43.71+j55.87	2.41+j16.26	SUB_B

On the base of the impedances from Table IV, the subroutine SUB_B remains selected as the valid one. It yields estimation of the fault distance (Fig. 5a) with around 0.5% error.

Quantitative evaluation of the presented fault location algorithm has been performed for very wide range of fault conditions. For faults involving earth the fault path resistance up to 30 Ω has been taken into account. Average fault location error was at the level of 0.5%, not exceeding 1%.

IV. CONCLUSIONS

Use of two-end synchronized measurements of three-phase currents accomplished by current differential protective relays, with additional incorporation of three-phase voltage from one line end, has been considered for practical fault location. This proposal for the fault locator input signals is aimed at incorporating the fault location function into the current differential protective relays. In this way the fault locator utilizes the communication infrastructure of the differential relays, thus not demanding additional communication links. As a result, the functionality of the differential relay is greatly increased. The presented method can be applied for both single-circuit and double-circuit series-compensated transmission lines.

The subroutines of the algorithm have been formulated with use of the generalized fault loop model, leading to the compact formulae. It is important that the distance to fault calculations do not involve source impedances and the pre-fault measurements. Thus, the main limitations of the one-end fault location algorithms are in simple way overcome.

The other important advantage of the developed algorithm relies on limiting the need for representing the compensating bank only for one subroutine (SUB_B). However, one can add the fault location function to the relays at both line ends and as a result of that the distance to fault is calculated without representing the bank at all.

Efficient procedure for selecting the valid subroutine has been presented as well. It allows reliable indication of the results, which are consistent with the actual fault.

The presented fault location algorithm has been thoroughly tested using signals taken from ATP-EMTP versatile simulations of faults on a series-compensated transmission line. The included example and the carried out evaluation with use of large number of the simulations show the validity and high accuracy of the presented fault location algorithm.

References

[1] IEEE Std C37.114: "IEEE guide for determining fault location on AC transmission and distribution lines," IEEE PES Publ., pp. 42, 2005.

[2] W.J. Cheong and R.K. Aggarwal, "A novel fault location technique based on current signals only for thyristor controlled series compensated transmission lines using wavelet analysis and self organising map neural networks," 8th IEE International Conference on Developments in Power System Protection, Amsterdam, vol. 1, 2004, pp. 224–227.

[3] J. Sadeh, N. Hadjsaid, A.M. Ranjbar and R. Feuillet, "Accurate fault location algorithm for series compensated transmission lines," IEEE Trans. on Power Delivery, vol. 15, No. 3, 2000, pp.1027–1033.

[4] M.M. Saha, J. Izykowski and E. Rosolowski, "Fault Location on Power Networks," Springer, London, 2010.

[5] M.M. Saha, J. Izykowski, E. Rosolowski, P. Balcerek and M. Fulczyk, "Accurate location of faults on series-compensated lines with use of two-end unsynchronised measurements," 9th IET International Conference on Developments in Power System Protection, Glasgow, 2008, pp. 338–343.

[6] M.M. Saha, J. Izykowski, E. Rosolowski and B. Kasztenny, "A new accurate fault locating algorithm for series compensated lines," IEEE Trans. on Power Delivery, vol. 14, No. 3, 1999, pp. 789–797.

[7] C.-S. Yu, C.-W. Liu, S.-L. Yu, and J.-A. Jiang, "A new PMU-based fault location algorithm for series compensated lines," IEEE Trans. on Power Delivery, vol. 17, No. 1, 2002, pp. 33–46.

[8] M.M. Saha, J. Izykowski and E. Rosolowski, "A fault location method for application with current differential protective relays of series-compensated transmission line," 10th IET International Conference on Developments in Power System Protection, Manchester, 2010, paper: 05.2.

[9] IEEE Std. C37.118: "IEEE standard for synchrophasors for power systems," IEEE PES Publ., 2006, pp. 65.

[10] H. Dommel, "ElectroMagnetic Transients Program," BPA, Portland, Oregon, 1986.